Ionospheric VHF Scattering Near the Magnetic Equator During the International Geophysical Year

Robert Cohen and Kenneth L. Bowles

Contribution From Central Radio Propagation Laboratory,
National Bureau of Standards, Boulder, Colo.

General results and statistical studies of equatorial VHF oblique ionospheric scatter signals are presented for one calendar year of the International Geophysical Year. The equatorial scatter signals were usually stronger than their counterparts at temperate latitudes. Scattering was observed comparable to the D-region scatter propagation familiar elsewhere, but usually the E-region scatter predominated. Scattering via F-region irregularities was observed at nighttime over a 2580 km path centered about the magnetic equator.

The intense daytime equatorial E-region scattering was established to be largely due to irregularities associated with the equatorial electrojet. Its communications potentialities appear promising for paths having midpoints within a 10° band of latitude centered about the magnetic equator.

When the D-region scattering was distinguishable, it usually appeared to be stronger than that over similar paths at temperate latitudes. However, during the daytime over a path centered just at the magnetic equator, this comparison is just the opposite.

Relatively strong scattering from irregularities in the E region was also observed at nighttime, with the result that the weakest signals received diurnally over the equatorial paths were comparable to the strongest signals propagated over similar paths at temperate latitudes.

Both the daytime and nighttime scattering via E-region irregularities exhibited an asymmetry about the magnetic equator, being stronger for a path midpoint 5° south of the magnetic equator than for a midpoint a similar distance to the north.

1. Introduction

During one calendar year (December 1957 through November 1958) of the International Geophysical Year, the National Bureau of Standards conducted observations of radio wave propagation near 50 Mc/s in the vicinity of the magnetic equator in South America. The mechanism of propagation was by scattering from electron density irregularities in the equatorial ionosphere, and a number of experimental paths were in operation. This kind of scattering has been referred to as "VHF Forward Scatter."

The oblique propagation technique is useful for observing the medium within a scattering volume defined by the intersection of the receiving and transmitting antenna beams and/or by the geometry of the scattering irregularities. The intensity and frequency spectrum of the received signal, upon being studied as functions of space and time, serve to determine various characteristics of the irregularities. The potentialities of this technique are enhanced when these observations are combined with other methods of monitoring the scatter-medium, such as with an ionospheric sounder at the path midpoint.

Near the magnetic equator, it is shown in the following that scattering of VHF radio waves can be supported by electron density irregularities having diverse origins. As at other latitudes, these can be turbulent irregularities in the D region (and/or meteoric ionization). Superimposed upon this background signal from turbulent scattering irregularities are signal components from a variety of irregularities in the E and F region. The origin of the latter irregularities is probably not turbulence. These irregularities are associated with the phenomena of "sporadic E" and "spread F" observed on ionospheric sounders. When such irregularities are present, the additional signal is usually comparable to or much stronger than the turbulent background signal. For convenience, propagation of the latter could be designated as "D scatter" propagation, and the terms "E scatter" and "F scatter" can be used to characterize propagation resulting from the other varieties of irregularities in the E and F regions.

The observations reported in this paper were obtained using a group of 50 Mc/s oblique ionospheric scatter circuits operated in the vicinity of the magnetic equator during the International Geophysical Year. Readers may refer to Bowles and Cohen [1957] for design details of these scatter circuits. Most of the circuits, for purposes of intercomparison, essentially duplicated experimental parameters employed in previous experiments at other latitudes [see Bailey, Bateman, and Kirby, 1955; Joint Technical Advisory Committee, 1960]. Briefly summarized, typical parameters were:

Path length	Roughly 1300 km.
Transmitter power	2 kw.
Antenna gain	23 db relative to free space dipole.
Receiver bandwidth	300 c/s.

This paper summarizes the general results of this equatorial scatter program, with emphasis on the statistics of signal strengths propagated over the various paths. The results of these studies contain information about the physics of the scattering irregularities, and about possible communications applications. Preliminary accounts of this work have been published by Gates [1959] and by the authors [Bowles and Cohen, 1960, 1962]. A detailed analysis of that portion of the propagation attributable to scattering in the F region has also appeared [Cohen and Bowles, 1961]. The propagation data described in this paper, along with certain of the basic analyses thereof, are available through the IGY World Data Centers.

The equatorial ionosphere is relatively abundant in electron density irregularities, both in the E and F regions. The present paper deals mainly with the oblique VHF scatter propagation supported by these irregularities, while the physical nature of the irregularities themselves is being treated in other papers.

The equatorial scatter signals (observed over paths comparable to those that have been studied at other latitudes) were usually stronger than their counterparts elsewhere. (It was established from ionosonde and oblique pulse data that this relatively strong scatter was associated with phenomena in the E region.) This scatter predominated over the weaker "turbulent" scattering occurring at lower heights, so that only in its absence was it possible to observe the weaker constituent of the total signal. At such times the turbulent background level, or D scatter, was usually stronger than that at temperate latitudes. However, there was some indication that this may not be the case in the daytime just at the equator (cf sec. 5.2). In any event, the signal level over equatorial paths scarcely ever fell below a microvolt, whereas over comparable paths in temperate latitudes the median signal seldom exceeds that level.

For a received signal strength (open circuit antenna voltage) of 1.0 μv (which is the reference voltage corresponding to 0 db), the attenuation of signal relative to inverse distance transmission (i.e., for a perfectly reflecting ionosphere) is 100 db for the Arequipa →Trujillo path to be discussed. This attenuation results from a calculation following the procedure of Bailey, Bateman, and Kirby [1955], and refers to a 50 ohm impedance at the receiver input terminals and to a power at the transmitting antenna of 2 kw. (The corresponding value for the Antofagasta →Huancayo transmission path is 98 db, and 100 db for Huancayo→Guayaquil). The signal strengths employed in the statistical analysis have been corrected for transmission line losses at both ends of the paths.

The daytime equatorial E region irregularities have been identified with the equatorial electrojet [Matsushita, 1951; Bowles and Cohen, 1962]. They are associated with the 'equatorial sporadic E' and "equatorial slant sporadic E" configurations on ionograms [Cohen, Bowles, and Calvert, 1962]. The strong daytime equatorial VHF scatter signals were found in these experiments to have time-variations corresponding to the time-variations of these con-

figurations (and of the horizontal intensity of the magnetic field), as observed at the magnetic equator. The physical connection of these electrojet-associated phenomena is discussed by Cohen and Bowles [1963].

Other varieties of sporadic E occur at night at the magnetic equator, and the corresponding irregularities support appreciable oblique scattering at VHF. Another nighttime phenomenon is the occurrence of spread F irregularities, and it has been demonstrated [Cohen and Bowles, 1961; Calvert and Cohen, 1961] that certain of these, the "equatorial spread F" irregularities, support F-scatter propagation.

2. Design of the Experiment

The major portion of this observing program has been the regular recording at various receiving locations of ionospherically scattered continuous wave signals emanating from three transmitters at about 50 Mc/s. The several paths that were involved are shown in figures 1 and 2. The paths to be discussed in this paper are those shown in figure 2, although parameters also are tabulated in table 1 regarding other experimental paths. (The Panama→Guayaquil path has been discussed elsewhere [Smith and Finney, 1960], while other paths not along the west
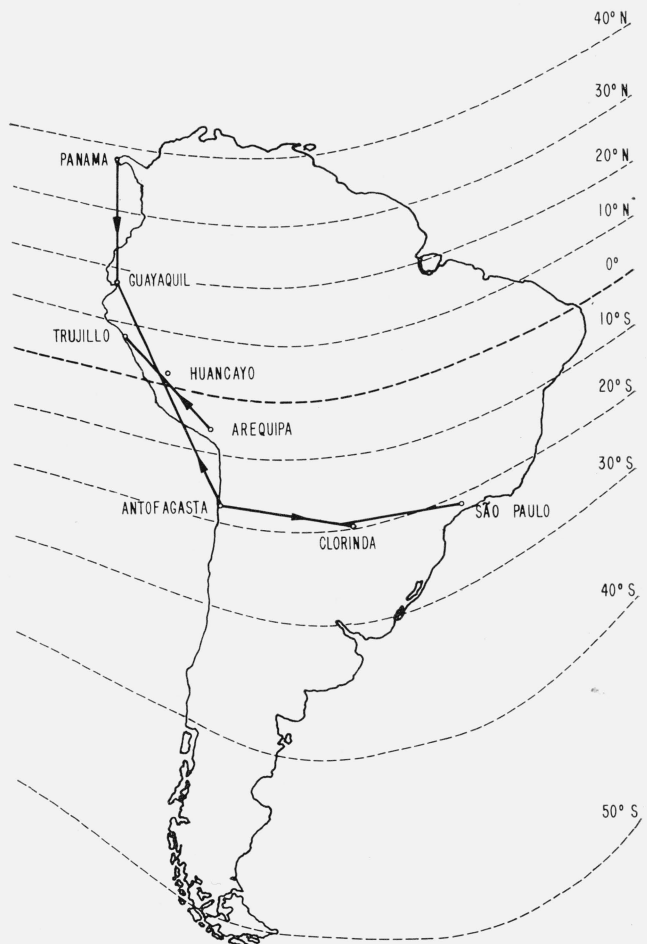

FIGURE 1.   *The deployment of IGY forward-scatter stations in South America relative to the magnetic isoclines.*
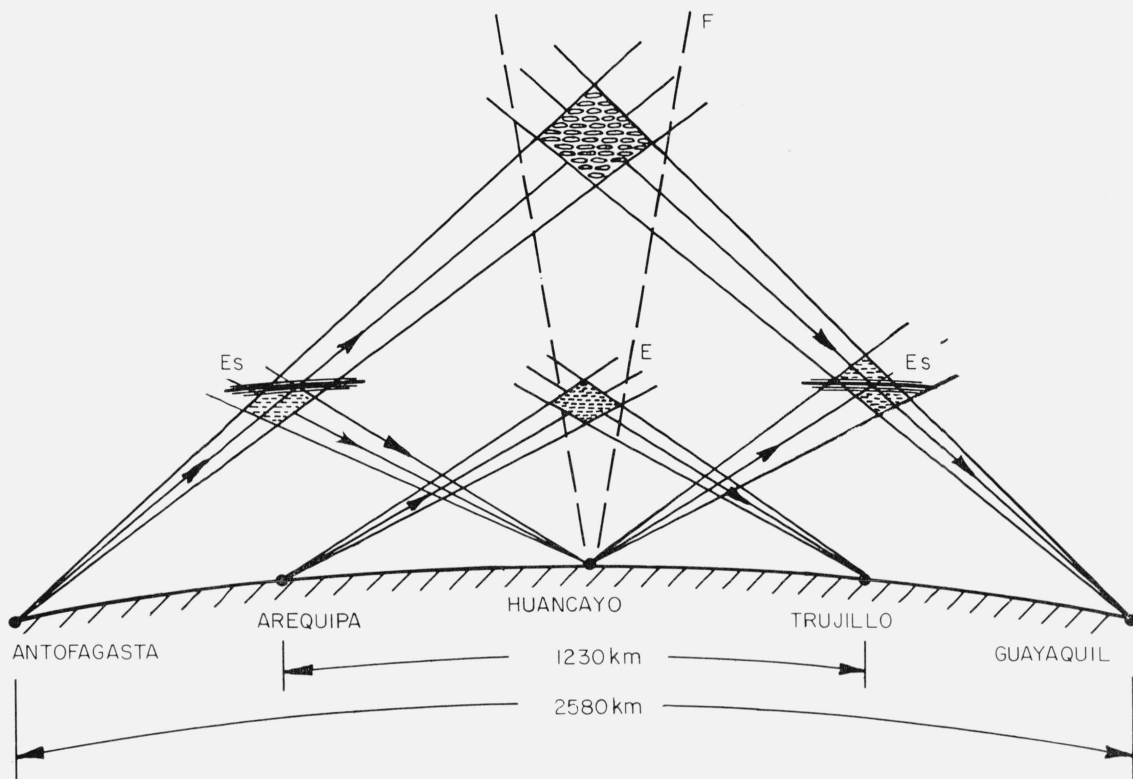
FIGURE 2. *Schematic diagram of the vertical cross sections of antenna beam intersections along the west coast of South America, indicating four of the propagation paths referred to in this paper.*

coast of South America (Antofagasta→Clorinda, Antofagasta→São Paulo) have not yet been analyzed). Because of difficulties in their interpretation, data for the "skew" paths (Antofagasta→Trujillo, Arequipa→Guayaquil) are not treated here, although statistical analyses for that propagation have been made.

The motivation for transmitting from south to north over the paths discussed here was the fact that great circles emanating from the transmitter locations intersect regions of Central and North America where numerous radio amateurs monitor the 6-m (50 Mc/s) band. The great circles corresponding to the Antofagasta and Arequipa antenna beams are shown in figures 3 and 4, which are mappings such that every radius is a great circle. (Radio amateurs have actually pioneered in the study of transequatorial propagation at VHF, and during the IGY their reports were collected and studied in connection with another project [Southworth, 1960].)

There were two basic transequatorial paths employed, Arequipa→Trujillo and Antofagasta→Guayaquil. The first path was to enable a comparison between the equatorial propagation and propagation over similar paths at temperate and arctic locations. (At those latitudes, such paths had been operated with transmitter-receiver separations of about 1200 km, comparable to the distance from Arequipa to Trujillo, and involved scattering in the D and lower E regions.) The second basic path was established to explore the possibility of scattering via the F region, while suppressing (insofar as possible) the scatter in the D and E regions by using a 2580 km transmitter-receiver separation.

The considerations in designing the F-scatter experiment are discussed by Cohen and Bowles [1961]. The presence of a transmitter in Antofagasta was exploited to attempt F scatter over the Antofagasta→São Paulo path, and also to study D and E scatter between Antofagasta and Clorinda, both these paths being parallel to the magnetic equator.

In view of the presence of transmitting and receiving stations appropriately located, and with the deployment of a third small transmitter at Huancayo, it was then possible to monitor the ionospheric scattering over four other paths (Antofagasta→Trujillo, Arequipa→Guayaquil, Antofagasta→Huancayo, Huancayo→Guayaquil), and thereby determine the latitudinal dependence of the equatorial phenomena to be observed. This dependence upon latitude provided an idea of the extent and symmetry about the magnetic equator of these phenomena. Transmission from Huancayo to Guayaquil, and the reception of Antofagasta signals at Huancayo enabled the observer to establish whether the Antofagasta→Guayaquil signal was arriving by F scatter or by a two-hop E scatter (via the earth in the neighborhood of Huancayo).

Figure 5 gives an indication of the portions of

Table 1. *Details regarding various experimental paths*

Transmitter→Receiver	ANF→TRU	ANF→GYE	ANF→HCO	HCO→GYE	ARQ→TRU	ARQ→GYE
Frequency (Mc/s)	49.960	49.960	49.960	49.880	49.920	49.920
Date of commencement	7 Dec. 1957	10 Dec. 1957	1 Dec. 1957	10 Dec. 1957	7 Dec. 1957	10 Dec. 1957
Date of termination	30 Nov. 1958	30 Nov. 1958	30 Nov. 1958	30 Nov. 1958	30 Nov. 1958	30 Nov. 1958
Coordinates of transmitting site.	Antofagasta, Chile 23°44' S; 70°15' W	Antofagasta, Chile 23°44' S; 70°15' W	Antofagasta, Chile 23°44' S; 70°15' W	Huancayo, Peru 12°2.7' S; 75°20.4' W	Arequipa, Peru 16°44' S; 71°52.5' W	Arequipa, Peru 16°44' S; 71°52.5' W
Coordinates of receiving site	Trujillo, Peru 8°6' S; 79°4.5' W	Guayaquil, Ecuador 2°36' S; 80°24' W	Huancayo, Peru 12°2.7' S; 75°20.4' W	Guayaquil, Ecuador 2°36' S; 80°24' W	Trujillo, Peru 8°6' S; 79°4.5' W	Guayaquil, Ecuador 2°36' S; 80°24' W
Surface path length-km (Great Circle).	1980	2580	1410	1180	1230	1830
Coordinates of path midpoint.		13°14' S; 75°31' W	17°54' S; 72°53' W	7°21' S; 77°52' W	12°21' S; 75°32' W	
Magnetic dip at path midpoint.		≈0°	≈8° S	≈10° N	≈2° N	
Azimuth of transmitter from receiver.	152.6°	156.0°	158.2°	152.4°	140.2°	149.9°
Azimuth of receiver from transmitter.	330.2°	333.7°	336.7°	331.8°	319.4°	328.4°
Actual antenna azimuth/location.	333.7°/ANF	156.0°/GYE	161.4°/HCO recvg	328.8°/HCO transg	141.6°/TRU	320.0°/ARQ

Transmitter→Receiver	ANF→CLO	ANF→SãoP	PAN→GYE	ANF→GYE via backscatter	ARQ→HCO	HCO→TRU
Frequency (Mc/s)	49.960	49.960	49.760	49.960	49.920	49.880
Date of commencement	27 Mar. 1958	7 Apr. 1958	30 Apr. 1958	28 Mar. 1958	11 Aug. 1958	29 Sep. 1958
Date of termination	29 Nov. 1958	30 Nov. 1958	16 Nov. 1958	6 Apr. 1958	30 Nov. 1958	5 Nov. 1958
Coordinates of transmitting site.	Antofagasta, Chile 23°44' S; 70°15' W	Antofagasta, Chile 23°44' S; 70°15' W	Panama 9°23' N; 79°53' W	Antofagasta, Chile 23°44' S; 70°15' W	Arequipa, Peru 16°44' S; 71°52.5' W	Huancayo, Peru 12°2.7' S; 75°20.4' W
Coordinates of receiving site	Clorinda, Argentina 25°20' S; 57°54' W	São Paulo, Brazil 23°33' S; 46°38' W	Guayaquil, Ecuador 2°36' S; 80°24' W	Guayaquil, Ecuador 2°36' S; 80°24' W	Huancayo, Peru 12°2.7' S; 75°20.4' W	Trujillo, Peru 8°6' S; 79°4.5' W
Surface path length-km (Great Circle).	1280	2390	1330	≥2580	640	600
Coordinates of path midpoint.	24°38' S; 64°2' W	24°6' S; 58°28' W	≈3°23' N; 80°8' W		≈14°23' S; 73°36' W	≈10°4' S; 77°12' W
Magnetic dip at path midpoint.	≈18° S	≈18° S	≈28° N		≈2° S	≈5° N
Azimuth of transmitter from receiver.	275.2°	264.8°	2.5°	156.0°	144.8°	137.4°
Azimuth of receiver from transmitter.	100.4°	94.3°	182.5°	333.7°	323.9°	316.8°
Actual antenna azimuth/location.	≈100°/ANF ≈275°/CLO	} ≈260°/S.P	182.5°/PAN	336°/GYE	{161.4°/HCO 320.0°/ARQ	328.8°/HCO 141.6°/TRU

ionosphere under scrutiny along the west-central coast of South America, as determined by the antenna-beam intersections for these four paths and for the two basic paths. They encompass 12° in latitude and 5° in longitude. The first segment of the diagram is for the two asymmetric or "skew" paths (Antofagasta→Trujillo, Arequipa→Guayaquil), the central segment for the three symmetric D- and E-scatter paths (Antofagasta→Huancayo, Arequipa→Trujillo, Huancayo→Guayaquil), and the last segment for the F-scatter path (Antofagasta→Guayaquil). The deployment of ionospheric sounders at Huancayo, Chimbote, Chiclayo, and Talara, Peru; and at La Paz, Bolivia, enabled the correlation of features on the ionograms and the characteristics of the signals propagated in these scattering regions.

3. Instrumentation

3.1. Antennas

Rhombic antennas were generally employed in this research, although in several instances pairs of vertically stacked five-element Yagi antennas were used. The basic characteristics of these antennas were the same as for the antennas described by Bailey, Bateman, and Kirby [1955]. Additional details regarding the antennas of interest here are given in table 2, and for the Antofagasta→Guayaquil path, by Cohen and Bowles [1961]. The computed gain relative to a half-wave dipole at the same height was 18 db for the rhombic antennas and 12 db

FIGURE 3. *Polar plot of the world centered about Antofagasta, Chile, showing coverage of the principal antenna beam.*

for the pairs of Yagis. Sites were chosen so that ground reflection would increase the effective gains of these antennas by 6 db in each case. Over paths in which Yagi antennas were used for transmitting and/or receiving, the signal levels have been appropriately compensated (by 6 or 12 db) in the analysis, as if rhombic antennas had been used throughout and the calculated (plane-wave) antenna gains had been realized. (These corrections are only approximate, since the difference in gain that can be realized at any instant also depends upon the spatial extent of the region via which scatter signals can be propagated between the transmitter and receiver locations.) The antennas were directed so as to con-

centrate attention at about 85 km for the short paths, and around 180 km (later, at 270 km) for the long path.

3.2. Transmitters

The transmitters utilized enabled continuous-wave transmissions at powers up to 20 kw, but inasmuch as large powers were seldom required to observe a signal, the usual power radiated was about 2 kw. Accordingly, the signal-intensities observed have all been adjusted with that power level as a reference. This represents a departure from the reference level of 30 kw used by Bailey, Bateman, and Kirby [1955]. Thus a comparison of their

463

TABLE 2. *Antenna design data*

Location	Transmitting antennas			Receiving antennas		
	ANF*	ARQ	HCO	HCO	TRU	GYE*
Kind of antenna	Rhombic	Rhombic	Pair of Yagis	Rhombic	Rhombic	Rhombic
Takeoff angle	2.8°	4.7°	4.7°	5.6°	4.6°	3.1°
Height (meters)	20.8	16.8	17.3	14.2	18.3	27.6
Leg length (meters)	150	150		150	150	150
Angle of rhombus at feed point	20°	19°		19°	19°	20.5°
Vertical beamwidth of the lowest lobe	3°	5°	5°	6°	5°	3°
Horizontal beamwidth	6°	6°	60°	6°	6°	6°

*The Antofagasta and Guayaquil rhombic antennas were lowered to 12.6 m and 13.8 m, respectively, on 28 September 1958, resulting in takeoff angles of 5.8° and 6.2°.

FIGURE 4. *Polar plot of the world centered about Arequipa, Peru, showing coverage of the principal antenna beam.*
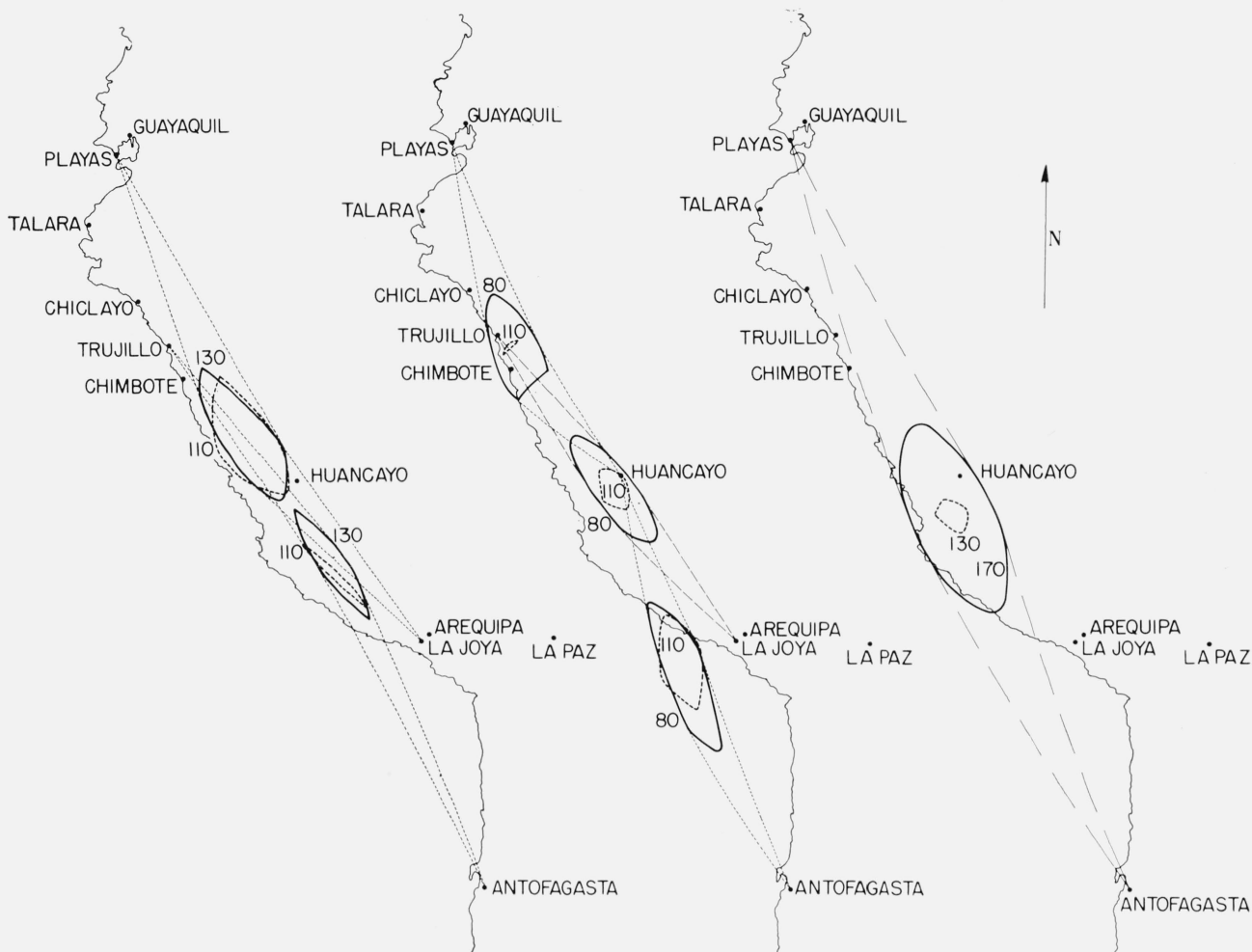
FIGURE 5. *The west coastal area of South America, showing the horizontal extent of the ionospheric volumes in which the antenna-beams intersect for the various combinations of receiving and transmitting stations.*

The contours are loci of points in the product antenna pattern that are 20 db weaker than the maximum "product-beam" sensitivity. (The numbers adjacent to the contours are the heights in kilometers for which loci were determined. The right-hand diagram is for the long path prior to lowering the antennas.)

signal-intensities with the present ones requires a compensation of about 12 db. The power radiated by each transmitter was continuously monitored at Antofagasta and Arequipa, and the Huancayo transmitted power was under frequent observation.

3.3. Receivers

NBS VHF receivers, designed especially for IGY applications by P. G. Sulzer and K. L. Bowles in 1956, were employed [Gray and Gorham, 1961]. They have relatively narrow bandwidths (100 or 300 c/s) and a dynamic range of about 100 db. The reference level employed was $1.0\mu v$ for a 50 ohm Thevenin equivalent generator without load, this level corresponding to 0 decibels. The AGC voltage resulting from the received signal was smoothed by an RC integrator having a 12 second time constant, and its magnitude was displayed versus time on a paper-tape chart moving at 3 in. per hour. The receiving systems were calibrated daily by use of standard signal generators. In spite of every effort to arrive at a significant measure of the absolute power received over the various paths, there are inherent errors in the precision to which this can be accomplished, and the tabulated signal intensities are probably subject to errors of ± 1 db at all levels, and to somewhat greater errors at especially high and low signal levels.

As customary in earlier VHF scatter observations, the transmissions were interrupted twice each hour to permit the external (usually cosmic) noise background level to be recorded, as a reference to the performance of the receiving system. (At freqencies around 50 Mc/s, cosmic noise predominates over receiver noise.)

During much of the calendar year of observations, the "fading rate" of certain received signals was monitored at Trujillo and Guayaquil. (The fading-rate recorder, designed in 1958 by B. B. Balsley and K. L. Bowles, utilized the detected signal from the receiver.) The fading-rate charts have a dynamic range extending from 0 c/s at the bottom to about
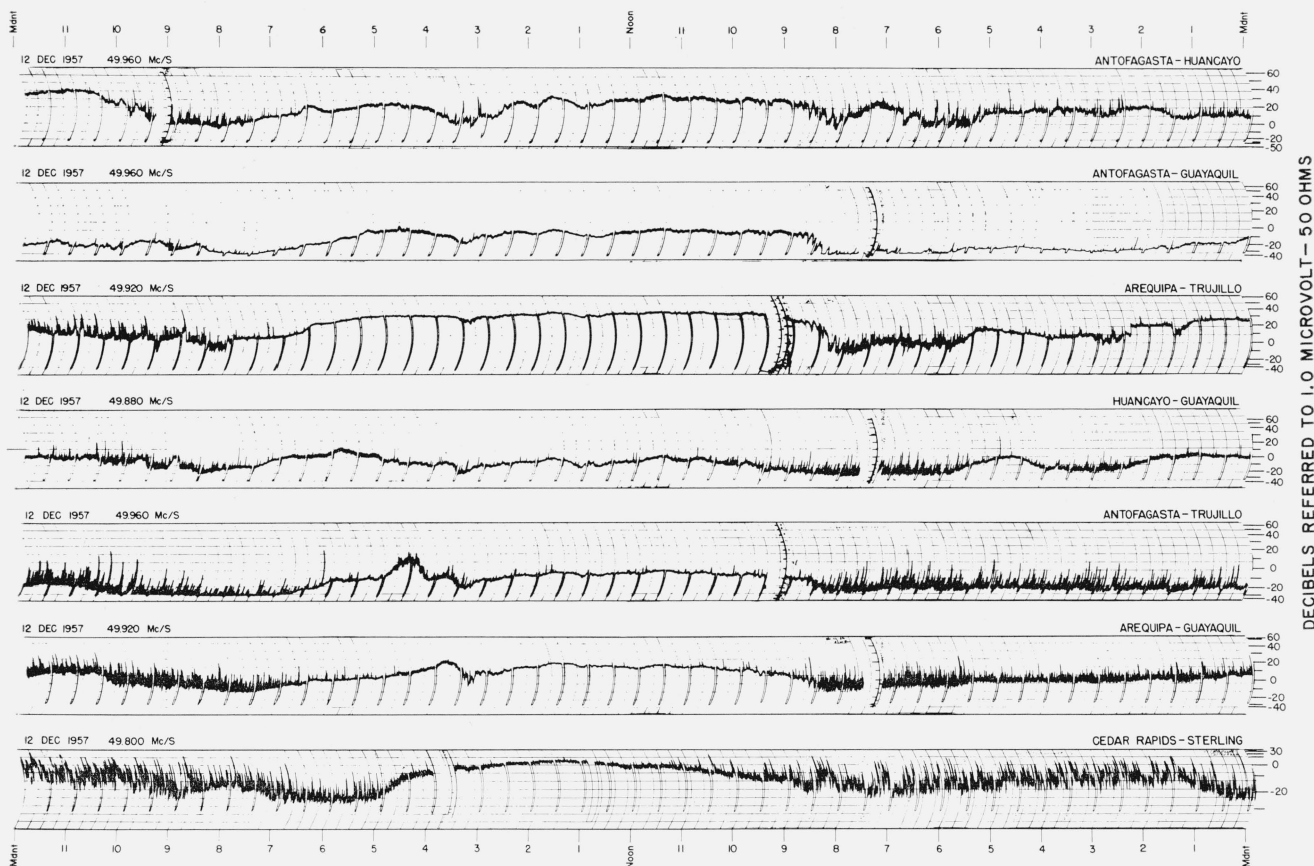
FIGURE 6. *A comparison for 12 December 1957 of the signal strengths near 50 Mc/s transmitted over the six paths described in this paper with those transmitted from Cedar Rapids, Iowa (41°52′ N; 91°41′ W) to Sterling, Va. (38°59′ N; 77°29′ W).*

The amplitudes are in decibels referred to one microvolt. The times stated are 75° W.

15 c/s at the top. They are calibrated with a sinusoidal signal as reference.

3.4. Special Experiments

Besides the routine monitoring of continuous wave transmission, special experiments were conducted using pulse modulation, voice modulation, and involving different antenna and receiving arrangements Some of the results of such experiments will be discussed in this paper.

4. Analysis of the Received Signals

4.1. Photographs

In order to provide ready acessibility to the strip-chart recordings (which are about 7 km in length, altogether), a photographic procedure was employed for displaying each day's records. This enables rapid, qualitative study and intercomparison, as well as correlation with other geophysical data. Inasmuch as it is particularly interesting to compare the radio records with the magnetic records from Huancayo, these have been photographed side by side. Certain radio records from NBS observations in the United States have been included as well,

to enable the comparison of equatorial signals with those at temperate latitudes, and with SID's and other worldwide geophysical phenomena. These photographs are available through the IGY World-Data Centers. Figure 6 is a photograph similar to those described. (Time in the original records increases from right to left, with 75° W. time being used.)

4.2. Signal Classification

A classification system has been adopted for dividing the signals into several categories according to the appearance of the record, and from other characteristics of the signal, such as its fading rate. An example of how well its fading rate can be used to characterize a signal is shown in figure 7, where a 3 hr portion of a signal and the associated rate of median crossings (fading rate) are compared. The signal strength record looks much the same during the first few hours, but its fading rate provides an "extra dimension" useful in distinguishing between the possible kinds of propagation being observed.

Figure 8 illustrates a portion of some signal recordings showing some of the characteristic signals that were obtained. The symbol "J" refers to a "jagged" or heterogeneous trace, "B" to a "bursty"
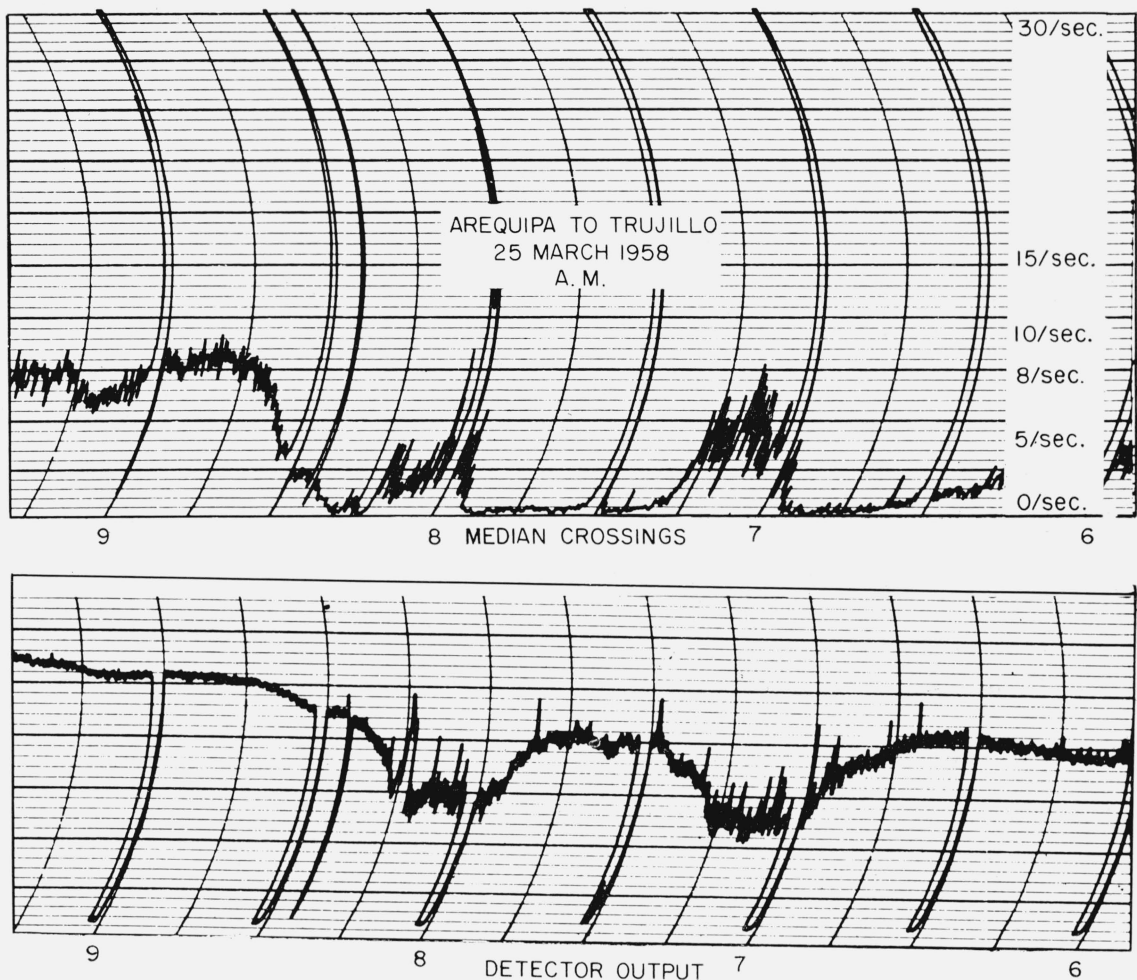
FIGURE 7. *A fading rate record (top) compared with the intensity variation (bottom) of the 50 Mc/s signal propagated from Arequipa to Trujillo, Peru between 0600 and 0930 hours on 25 March 1958.*

Time (75° W) progresses from right to left, and the detector output is roughly linear in decibels for the portion of chart shown.

or "bistatic" trace, and "M" to a "meteoric" trace. ("Bistatic" refers to a frequent tendency for the propagation to alternate fairly rapidly between relatively strong and weak modes.) The symbol "*F*," for "fine" (that could be applied to describe the high-level Arequipa→Trujillo signal in fig. 8), is a fourth designation, and pertains to a relatively flat, thin trace associated with a signal having a high fading rate. This same sort of trace, but having an arbitrary width of 4 db or more, has been called "W," corresponding to "wide." This choice of symbols was partly determined for compatability with automatic data processing equipment.

4.3. Tabulation of Signal Characteristics

In view of the relatively rapid variability of the scatter signals observed over the equatorial network, it was decided to measure their intensity at 5 min intervals. (The receiver calibration curves determined in the field were subjected to a smoothing process for levels corresponding to low signal strength before being used for this analog to digital conversion.) The measured intensities were recorded on punched cards, along with the cosmic noise levels and the classification of the signal into one of the five categories described above. The resulting cards were then processed so as to adjust the signal intensities to absolute levels. (This correction program accounted for variations in transmitter power, differences in antennas, and the calculable amount of noise contamination present at low signal-to-noise ratios.) The absolute levels so obtained are available from the IGY World Data Centers.

4.4. Statistical Analysis of the Absolute Signal Intensities

For statistical analyses the information on the punched cards was transferred to magnetic computer tape. Once having obtained a set of absolute signal intensities on magnetic tape, it became possible to accomplish very rapidly many kinds of statistical and correlation studies of the compiled data. One of the basic signal statistics that have been calculated in-
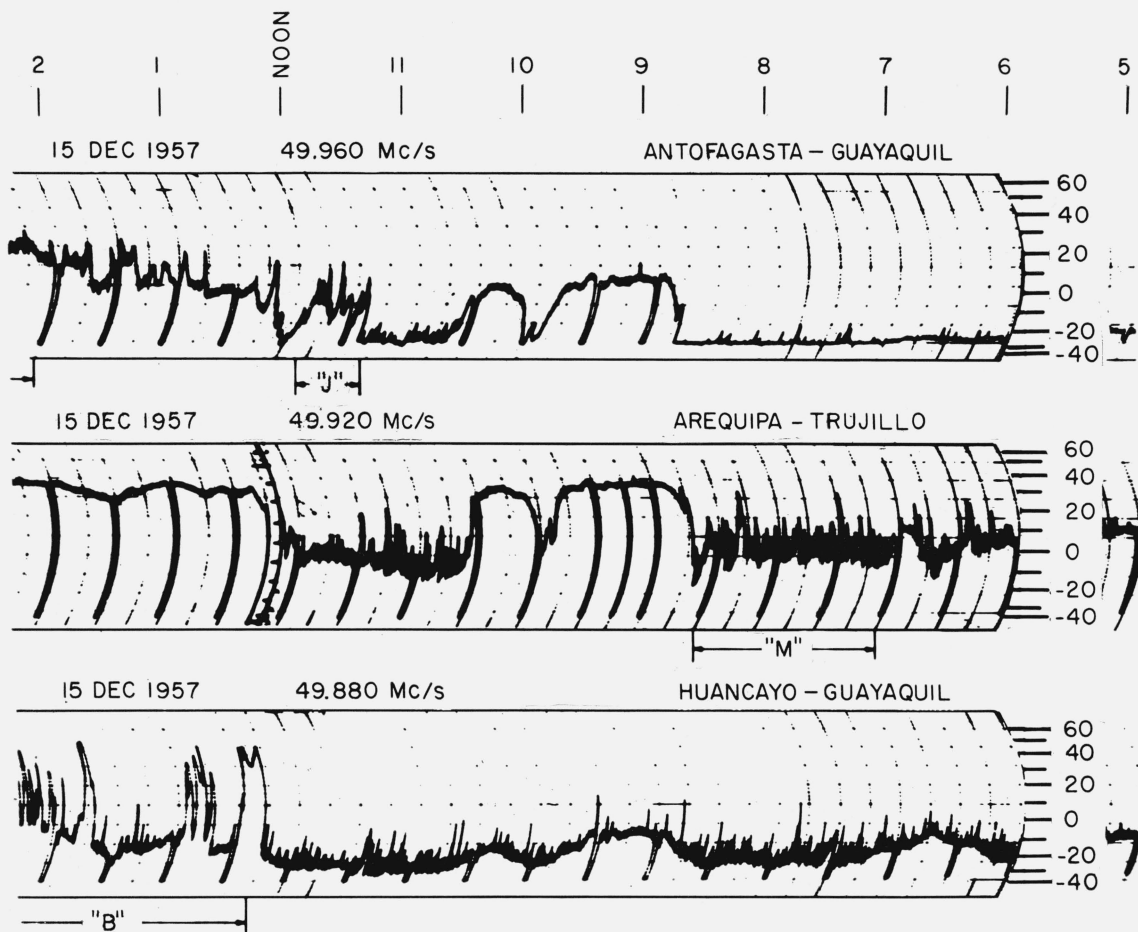
FIGURE 8. *Some sample signal recordings for 15 December 1957 illustrating the "J," "B," and "M" classifications described in the text.*

volved grouping the data (independent of class) into hourly units for a given month, and determining the decibel levels equalled or exceeded for various percentages of the time. (The times correspond to those about which the 1-hr intervals were centered.) The 0, 5, 10, . . ., 100 percentiles that were tabulated in this way for the six paths have been submitted to the IGY World Data Centers.

5. Characteristics of the Received Signals

5.1. General Description

As can be seen in figure 6, the scatter signals propagated near the equator were generally quite strong by comparison with the temperate latitude signals, shown here for the Cedar Rapids, Iowa→Sterling, Virginia path. (In this comparison, it should be noted that the calibration of the amplitudes is distinct in the equatorial and temperate latitude cases.) It was also apparent that there was relatively little observation near the equator of the meteoric trace characteristic of the temperate latitude turbulent propagation. On the short equatorial paths, the minimum scattered intensity during

most 24-hr periods was comparable to the maximum diurnal signal (usually attained at noon) observed at temperate latitudes.

The daytime equatorial records had fading rates considerably higher than were customary at temperate latitudes, and this accounts for the relatively fine traces shown in figure 6. Whereas the typical daytime fading rates observed at the equator are about 8 c/s, as shown in figure 7, those corresponding to temperate latitudes range between 0.2 and 5 c/s [Bailey, Bateman, and Kirby, 1955].

5.2. Turbulent Scatter Near the Magnetic Equator

Insofar as it is possible to isolate the turbulent scatter component over the three symmetric D and E scatter paths by selecting the classes of data described above as "meteoric" and "jagged," statistical analyses have been made to determine the diurnal variation of the median "turbulent" signal for each month. The corresponding signals obtained over a comparable temperate latitude path by Blair [1959] are plotted with these results in figure 9. Subsequent VHF studies by Blair and his colleagues have been described by Blair, Davis, and Kirby [1961].
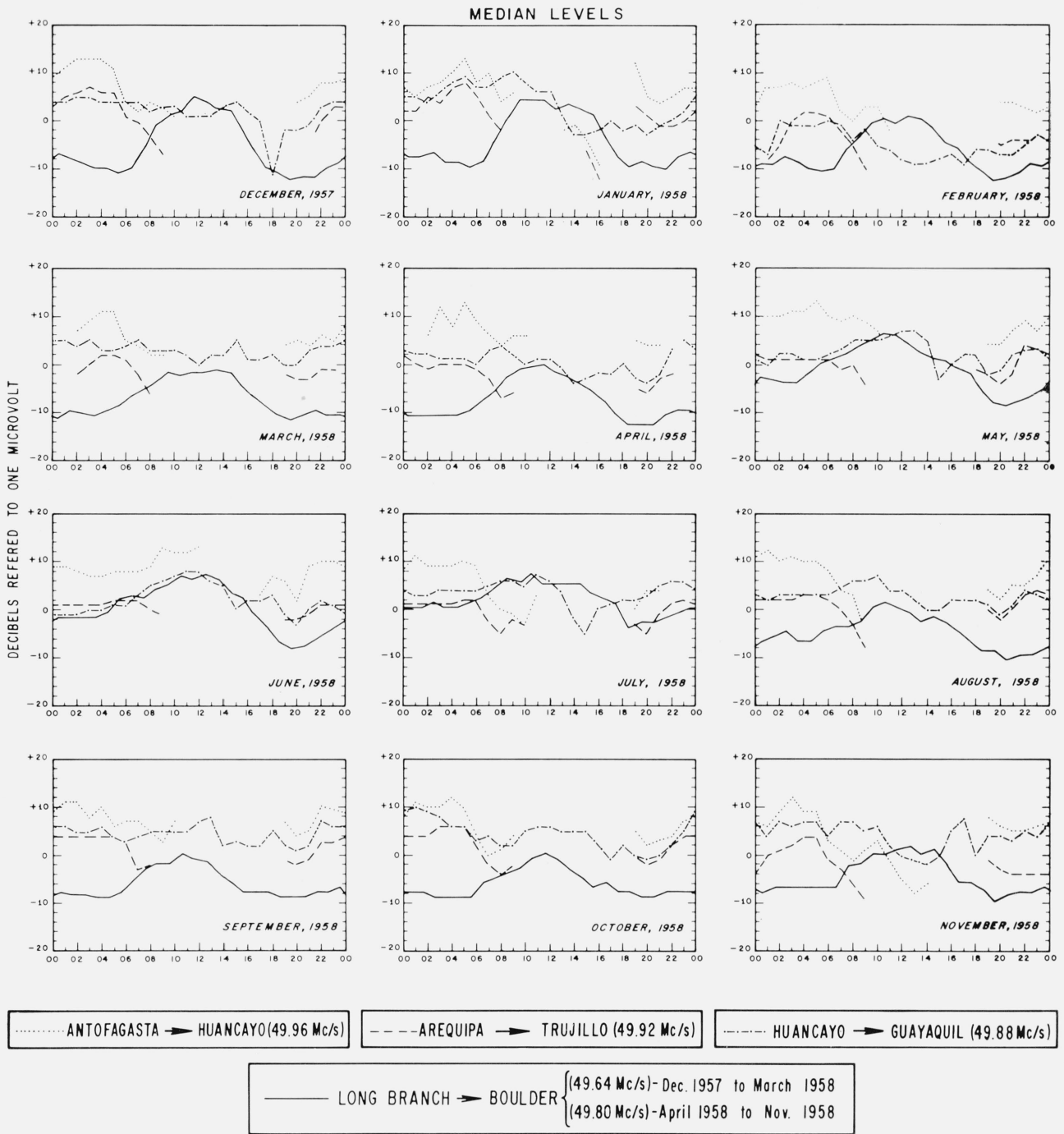
FIGURE 9. *The diurnal variation of monthly median "turbulent" signals over the "south," "central," and "north" paths compared with those over a temperate-latitude path from Long Branch, Ill. (40°13′ N; 90°01′ W) to Boulder, Colo. (40°08′ N; 105°15′ W).*

Local time at the receiving station is employed throughout, being 75° W for the equatorial paths and 105° N for the temperate-latitude path.

It is undoubtedly the case that the results for the equatorial turbulent scatter component are higher than they should be, due to the difficulty of isolating cases where only *D*-scatter propagation was involved. Also, only a limited number of samples was available for each month, and when that number became insignificantly small, no values were plotted. Never-

theless, it is apparent that even with considerable compensation for this difficulty, the nighttime signals that can be ascribed to turbulent scatter seem to be considerably higher than those observed at temperate latitudes, except during June and July 1958.

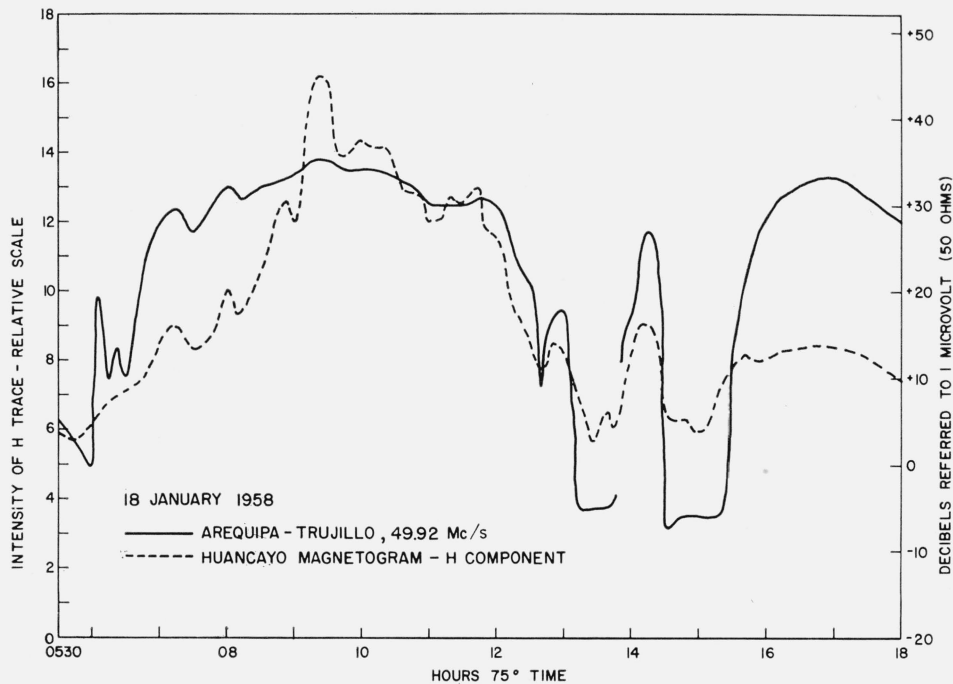It is more difficult to draw a conclusion for the daytime, when *E* scatter usually swamped the turbu-

FIGURE 10. *A comparison for 18 January 1958 of the relative intensity above the baseline of the horizontal magnetic field strength at Huancayo with the smoothed 49.92 Mc/s signal strength propagated over the Arequipa to Trujillo, Peru path.*

lent component of the scatter signal. However, from the statistics deducible during the limited periods when the *E* scatter was absent (such as occurs from time to time, as shown in fig. 8), it is perhaps possible to conclude that just south and north of the equator, judging from the Antofagasta→Huancayo and Huancayo→Guayaquil results, the propagation is more or less comparable to that at temperate latitudes, while right at the equator, judging from the Arequipa→Trujillo results, the *D* scatter seems to be considerably weaker. This is an interesting tentative conclusion that needs to be challenged by further observations. (Further mention in this paper of these three equatorial paths may refer to them, for brevity, as the "south," "central", and "north" path, respectively.)

5.3. Scattering Via the Equatorial Electrojet

Inasmuch as *D* scatter seldom predominated near the equator, it became important to establish what one could as to the mechanism of propagation of the strong scatter signals. This was relatively easy to do for the strong daytime signals, which frequently varied together over all six paths, as shown (for three of the paths) in figure 8. This "modulation" of the signal intensity thus corresponded to a large latitudinal region of the ionosphere, as apparent from figure 5.

It was immediately suspected that this daytime behavior was related to the equatorial electrojet and to the associated "equatorial sporadic *E*" irregularities that had been observed at Huancayo. It was soon established from a study of the Huancayo ionograms and magnetograms that this was indeed the

case. In fact, during times in which the modulation effects were observed simutaneously over a number of the paths, there was always a comparable modulation of the horizontal component of the earth's field as recorded by the Huancayo magnetogram. (This is illustrated in fig. 10.) At times when this modulation was particularly strong and deep, it could also be associated with the disappearance and reappearance of the equatorial sporadic *E* configuration on the Huancayo sounder, as occurred at the times of the deep daytime minima in figures 8 and 10.

The detailed association of the daytime signals over the Arequipa→Trujillo path with the variation of the horizontal magnetic field at Huancayo and the results of other experiments have led to some interesting conclusions regarding the nature and mechanism of formation of the "equatorial sporadic *E*" irregularities. These results are treated separately [Bowles et al., 1960; Bowles and Cohen, 1962; Farley, 1963; Bowles, Balsley, and Cohen, 1963; Cohen and Bowles, 1963]. It is important to point out in this connection that the intensity of this scatter signal is a quantitative measure of strength and/or numerosity of these irregularities.

All classes of signal over the various paths have been grouped together for the basic statistical analysis of the equatorial data. It is possible to study certain space and time features of the electrojet-associated *E* scatter from a presentation of these results as plotted in figure 11. This is a monthy comparison of median values for all signals propagated over the south, central and north paths, along with the corresponding statistics for a temperate latitude path. From this figure, one can get an idea of the latitudinal variation about the equa-
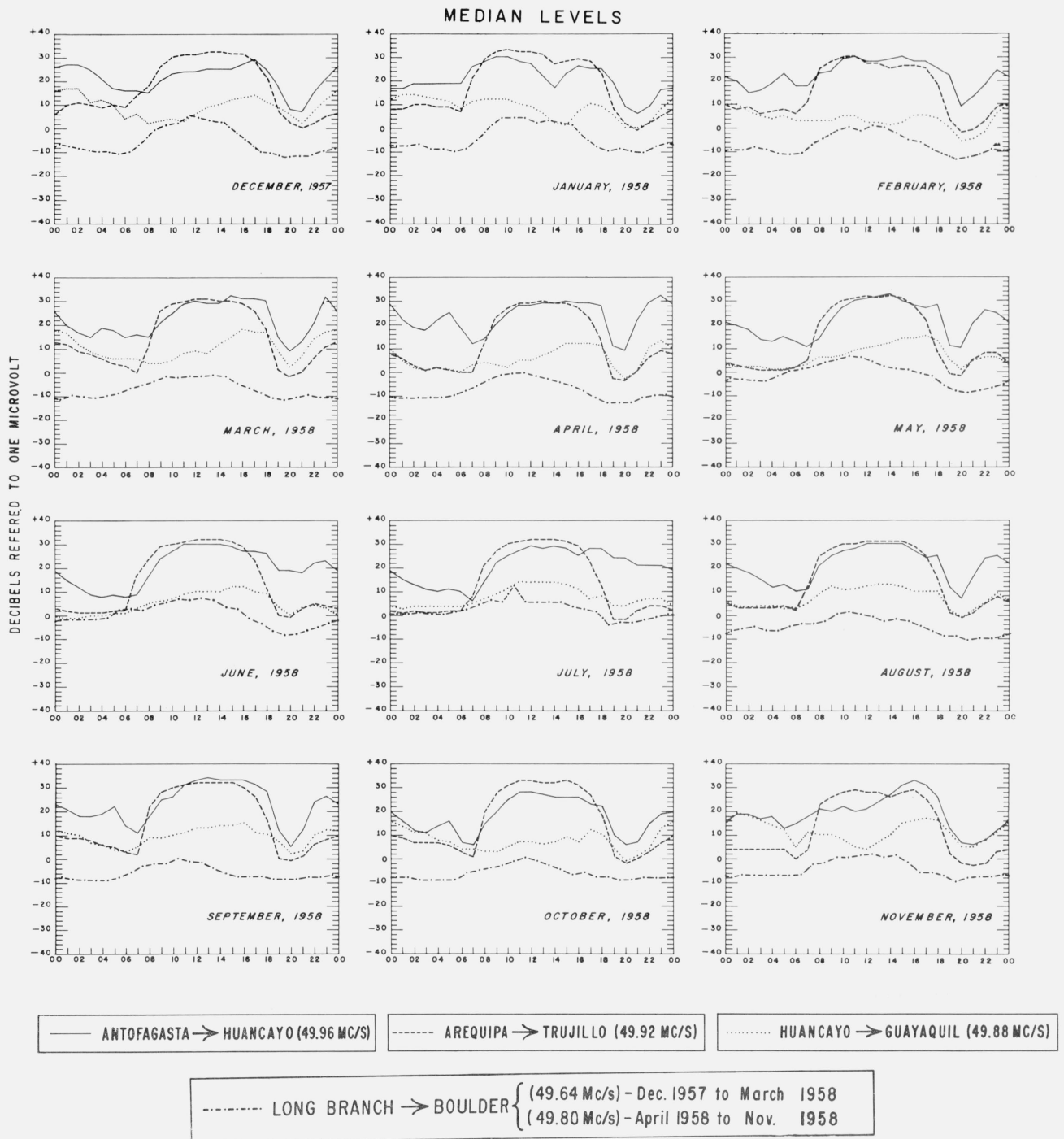
470

FIGURE 11. *The diurnal variation of monthly median signals (of all classes) propagated over the south, central and north paths, along with the corresponding statistics for all signals propagated over a temperate latitude path.*

Local time at the receiving station is employed throughout, being 75° W for the equatorial paths and 105° N for the temperate-latitude path.

tor of the electrojet-associated propagation, and of its diurnal and seasonal characteristics. (In an earlier publication [Bowles and Cohen, 1962], two of the curves in fig. 7 are in error and should be replaced by the appropriate curves from fig. 11.)

An immediate conclusion that one can draw is that there is a marked asymmetry about the mag-

netic equator, in that the signals over the south path were almost always considerably stronger than those over the north path, and comparable to (and at times higher than) those over the central path. There was apparently little effect of season in the comparisons of daytime medians, although there is evidence of an afternoon decrease in January 1958.
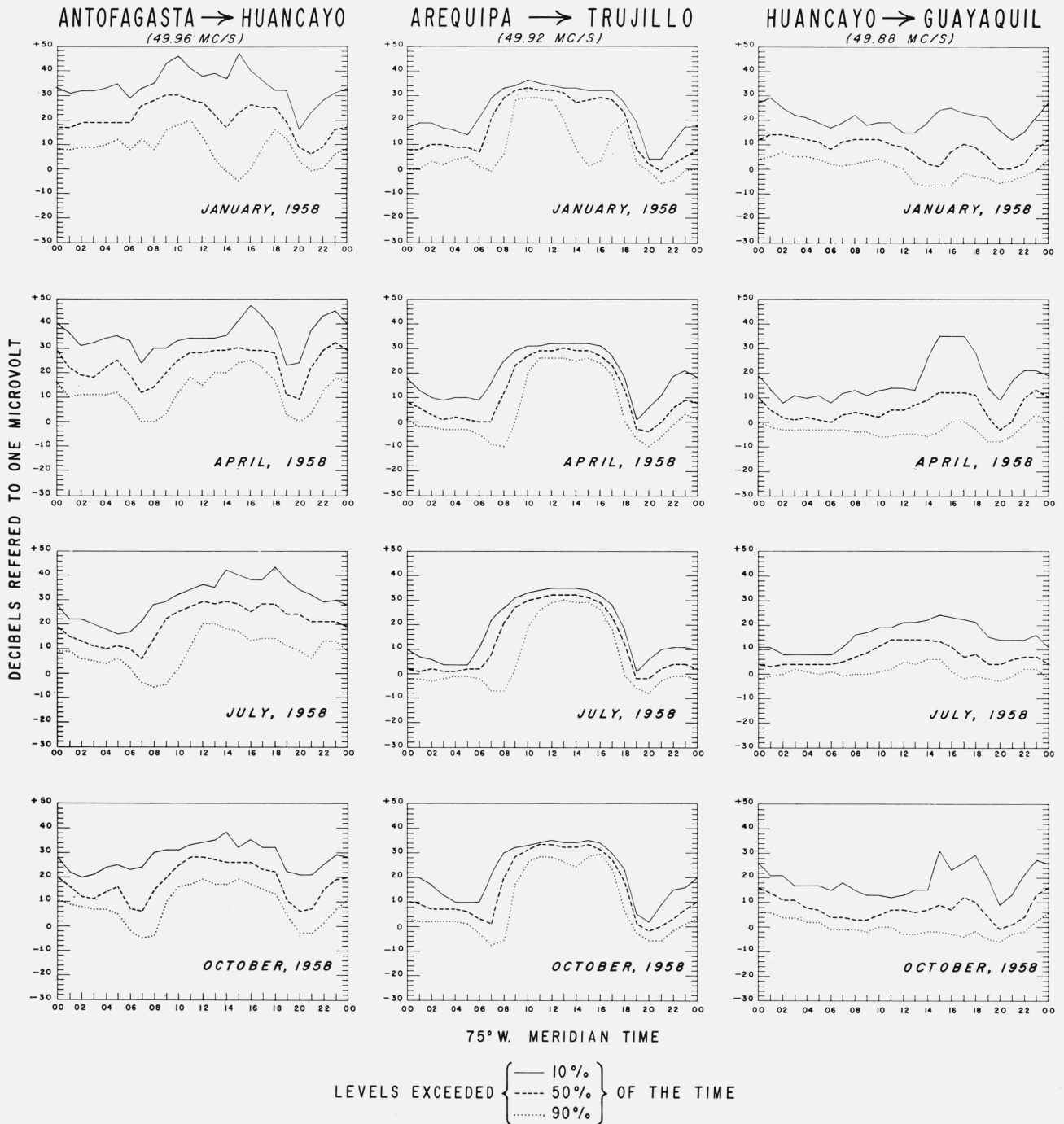
FIGURE 12. *The diurnal variation of the 10, 50, and 90 percentile signal levels over the south, central, and north paths for January, April, July, and October, 1958.*

A measure of the spread in signal levels is available from figure 12, in which the 10 and 90 percentiles are plotted along with the medians for 4 of the 12 months. There was very little fluctuation in the signal over the central path, even seasonally, although the weakest signals did show a minimum in the afternoon during summertime. There was apparently greater fluctuation in the morning hours than in the sunset decay period, which is because the decay is quite smooth and regular compared with the erratic growth of the electrojet propagation in the morning. There was greater spread in the signals over the other paths.
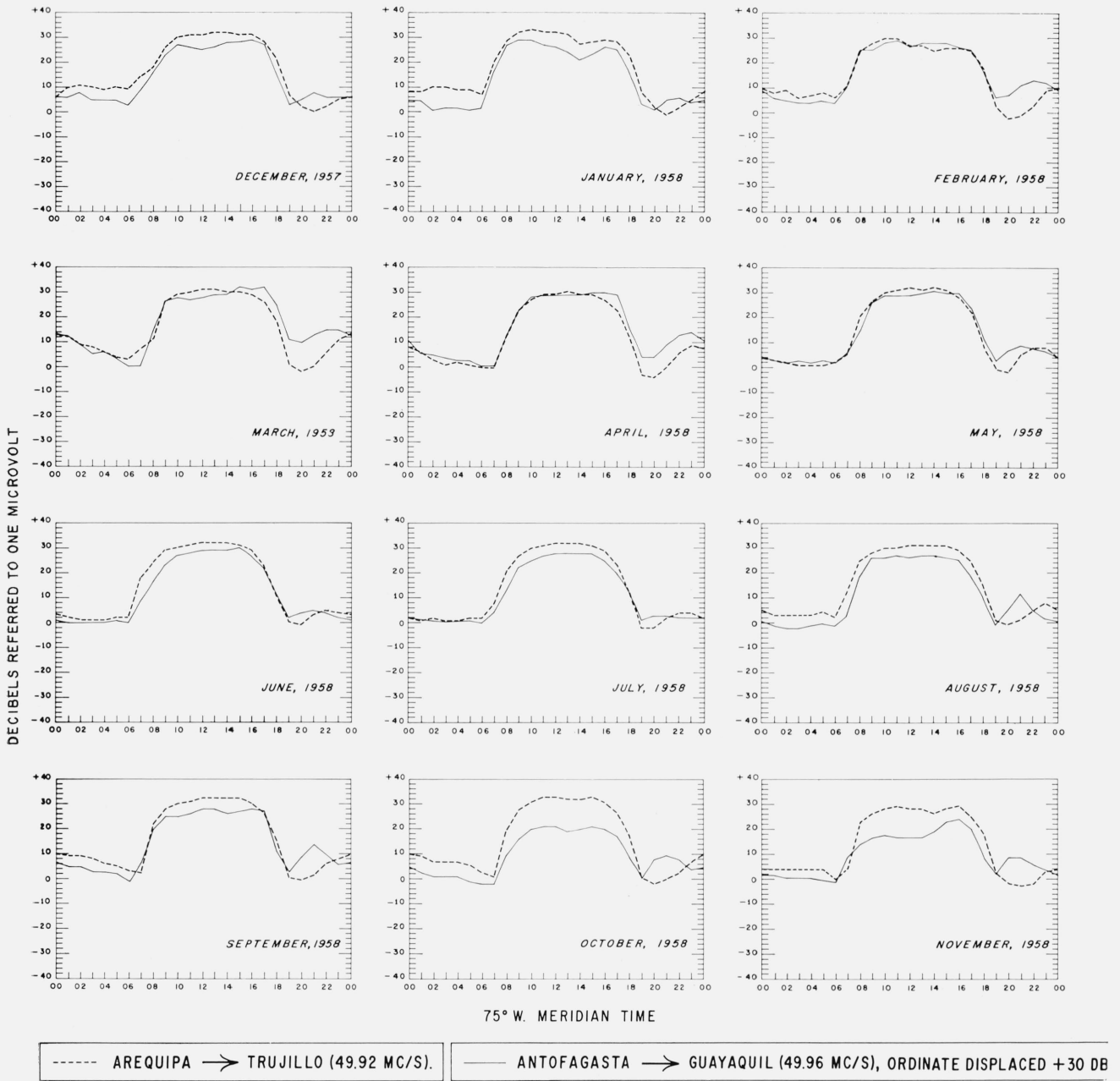
472

FIGURE 13. *The diurnal variation of monthly median signals (of all classes) propagated over the basic paths ("long" and "central" paths).*

5.4. F-Scatter Propagation

Figure 13 compares the median signal statistics over the "long" path (Antofagasta→Guayaquil) with those over the central path. It is apparent that during the daytime, scatter propagation via the electrojet was occurring over the long path, in spite of the horizon cutoff at about 120 km imposed by the 2580 km transmitter-receiver separation. However, as can be noted in figure 13, this signal was some 30 to 40 db weaker than the signal over the

central path, and its propagation is attributed to diffraction effects.

However, these statistics do indicate that there is an evening "hump" in the long-path propagation that does not appear over the central path, and this has been shown by pulse-height studies and by detailed correspondence with the Huancayo ionograms [Cohen and Bowles, 1961] to be attributable to F-scatter propagation. There was no evidence for the occurrence of F-scatter propagation on any path other than the long one.
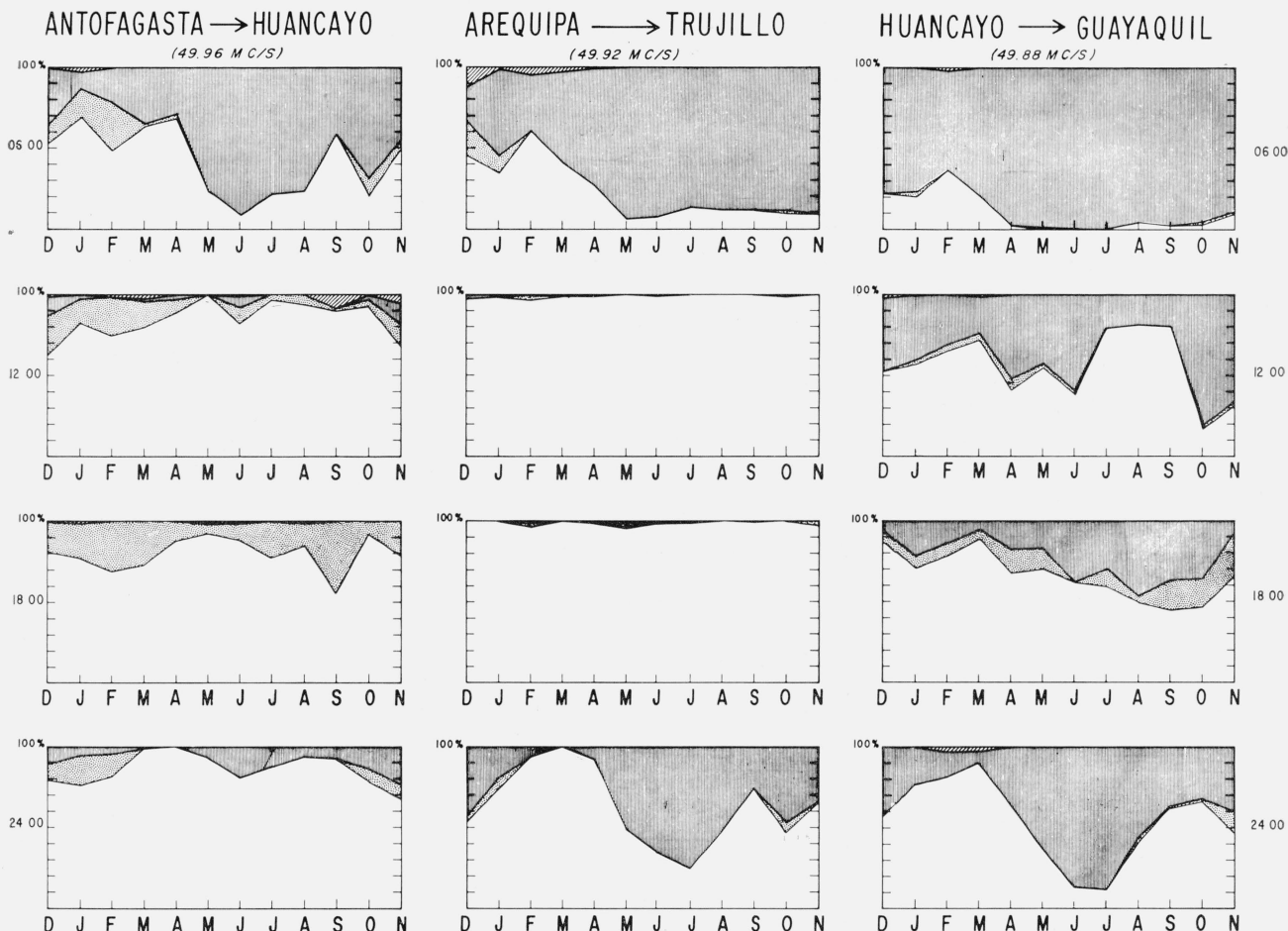
473

FIGURE 14. *The seasonal distribution among the five signal categories of the propagation over the south, central and north paths, for 06, 12, 18, and 24 hours local time (75° W).*

5.5. Nighttime Propagation by *E*-Region Scattering

The fact that figure 11 shows relatively high medians, even at night, in comparison with temperate latitude scatter, suggests the presence of a large amount of sporadic E irregularities at night. From pulse studies conducted over the Arequipa→Trujillo path it was established that the strong scatter propagation was always supported by irregularities between 90 and 110 km in height both by day and by night. However, the associated sporadic E irregularities were not readily apparent on the nighttime Huancayo ionograms.

Furthermore, the nighttime propagation over the south path was quite strong, and at midnight, as can be noted from figures 11 and 12, it reached strengths approaching the noontime levels. This was also true of the signal over the north path which, although not changing much diurnally, tended to reach a maximum at midnight. For the central path there were also relatively high signals at midnight.

It is interesting to note from figures 11, 12, and 13 that, as at temperate latitudes, there was a general tendency to reach a minimum at about 2000 local time, although over the long path, as a result of F scatter, this minimum occurred slightly earlier.

This strong scattering in the nighttime equatorial E region needs further study, inasmuch as little is known from ionograms about the irregularities that occur in the equatorial E region at night.

	+ 1 to + 5 db
	+ 6 to +10 db
	+ 11 to +15 db
	+ 16 to +20 db
	+ 21 to +25 db
	+ 26 to +30 db
	+ 31 to +35 db

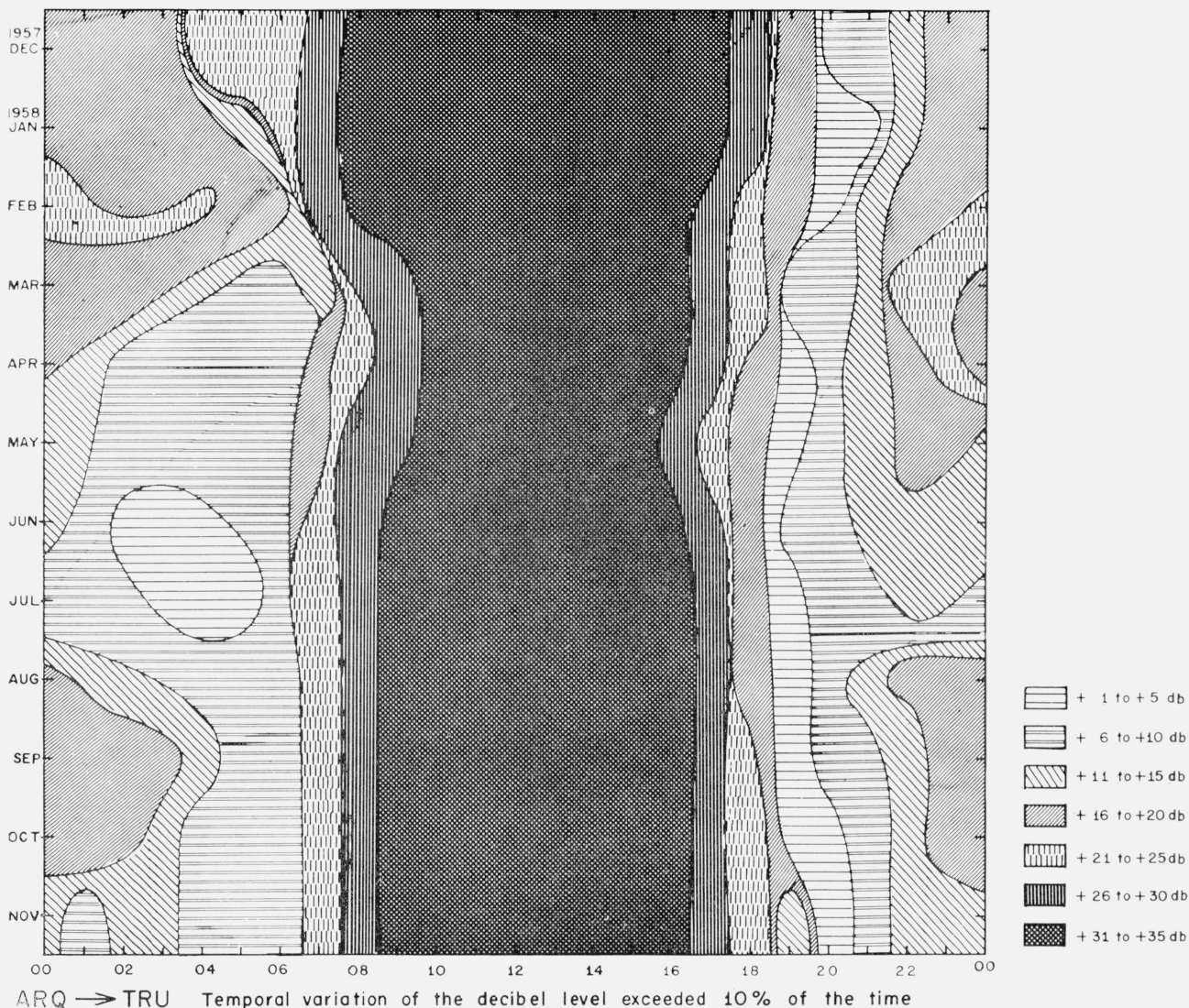ARQ ⟶ TRU Temporal variation of the decibel level exceeded 10% of the time

FIGURE 15. *Contours showing the temporal and seasonal variation of the range of signal strength exceeded 10 percent of the time over the central path.*

5.6. Seasonal Distribution of Scatter Signals Among the Several Classes

A statistical grouping among the five signal categories described earlier has been made for the propagation over the south, central, and north paths, for various times of the day, and is plotted as a function of the month in figure 14. As before, the two categories "M" and "J" have been grouped into a "turbulent" ("T") classification. The "F" category is associated with signals of relatively rapid fading rate, as for the electrojet propagation, while the wide-trace ("W") signal is characteristic of some of the nighttime varieties of *E*-region scattering.

5.7. Temporal and Seasonal Variations of the Equatorial Scattering

The contour plots of figures 15, 16, and 17 give an overall idea of the signal strength variation over the central path as a function of time of day and season. They pertain to the upper 10 percentile,

the lower 10 percentile, and the median signals, respectively. There is a characteristic diurnal cycle in each case, and this was apparently little affected by season, although the lowest daytime signals were weaker in January, February, and November than at other times of the year.

The median results of figure 17 for the central path can be compared with the more varied results over the south and north paths, presented in figures 18 and 19, respectively. At this time we offer no physical interpretation of the contours given in these figures. There are comparable contours available for IGY scatter propagation in the Far East [Tao et al., 1961].

5.8. Propagation by "Blanketing Sporadic *E*" Irregularities

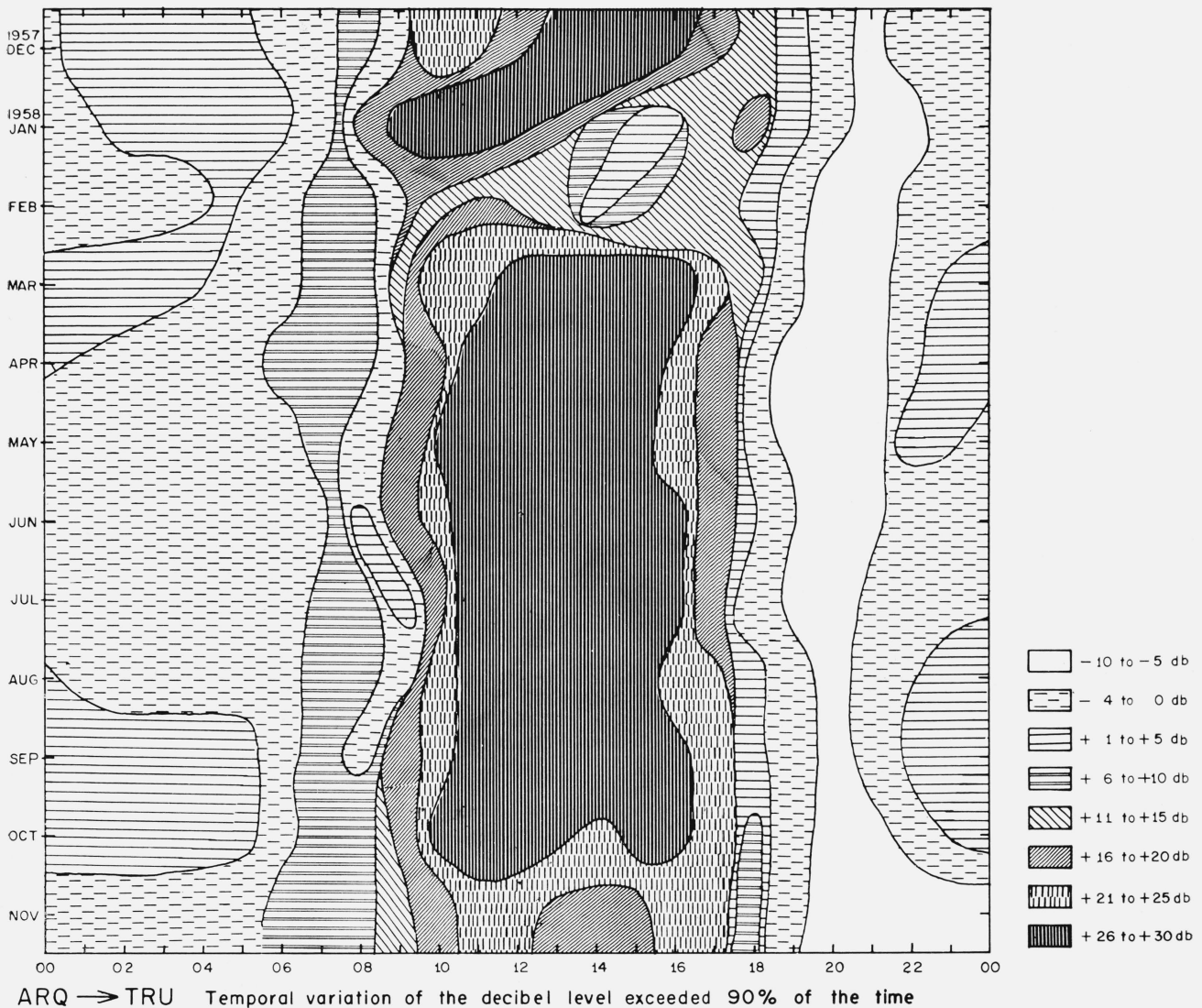Very strong daytime signals were frequently recorded (usually in the late afternoon) over the

FIGURE 16. *Contours showing the temporal and seasonal variation of the range of signal strength exceeded 90 percent of the time over the central path.*

north and south paths, similar to those associated with "blanketing sporadic E" irregularities at temperate latitudes. However, such signals did not occur over the central scatter path. That this observation is borne out on a statistical basis can be established by consulting the upper ten-percentile curves of figure 12, in which late afternoon peaks occur on the curves for the south and north paths but not on those for the central path. For some reason there appears to be a zone in the immediate vicinity of the magnetic equator where the blanketing sporadic E irregularities are not observed. A similar effect has been noted from standard ionograms by Knecht and McDuffie [1962].

5.9. Height of the Irregularities

Unidirectional pulse measurements were recorded in November 1958, for about 10 days on the central

path and during about 2 weeks over the long path. Absolute scatter heights could not be obtained solely from such measurements, but there was sufficient time-resolution to estimate the thickness of the scattering layers involved. Further details regarding the F-scatter pulse-observations have already been published [Cohen and Bowles, 1961]. By reference to the minimum time delay at which meteors were observable over the central path, *assuming* that delay to correspond to a height of 90 km, the daytime electrojet-associated propagation was estimated to arise from a height-interval of about 95 to about 100 km.

5.10. SID Effects

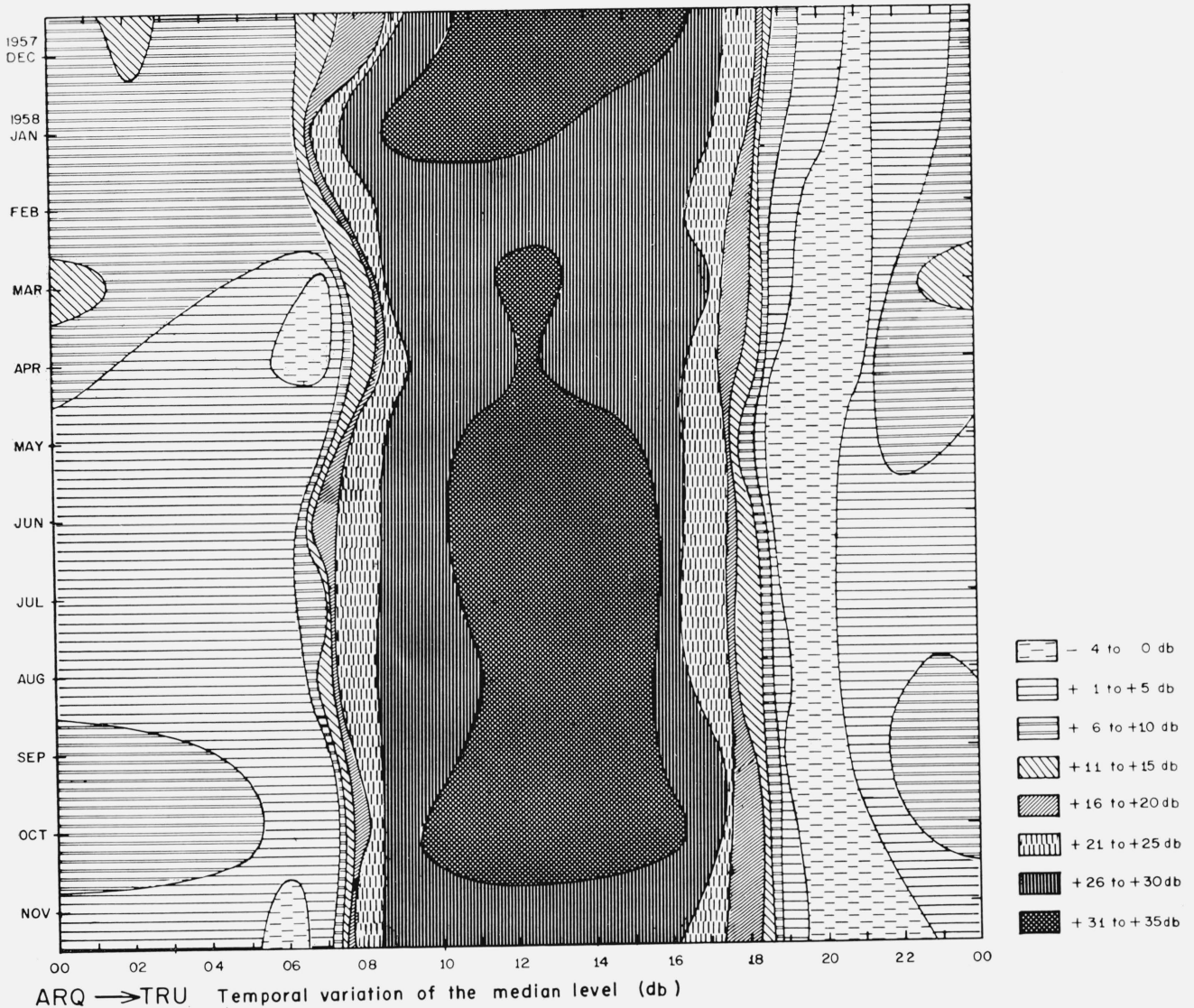Sudden ionospheric disturbances (SID's) seem to produce increased absorption of the 50 Mc/s equa-

476

FIGURE 17. *Contours showing the temporal and seasonal variation of the range of signal strength exceeded 50 percent of the time over the central path.*

torial scatter signals, without a concurrent increase in scattering. This is in contradistinction to the scatter observations at temperate latitudes, where a signal *enhancement* is usually associated with an SID.

The explanation of this difference between the two regions is presumably because the scattering volume at temperate latitudes is at a lower height than that for the preponderantly *E*-region scatter in the equatorial case. This means that a scatter-propagated wave will not traverse as much of the region of enhanced absorption in the temperate case as in the equatorial case. Thus, at temperate latitudes, the scattering phenomenon is enhanced sufficiently so that the increase in scattering overrides the extra absorption losses, while the reverse is true at equatorial latitudes.

The fading rate of the equatorial signals tended to increase during the presence of SID's.

Strong SID's were frequently noted at the equator when little or no effect was noted at temperate latitudes, and vice versa. The scattering volumes under comparison were roughly within 2 hr of longitude, and their latitudes differed by about 47° to 58°. The question of whether these comparisons may depend upon the relative solar zenith angles has not been examined. We offer no explanation for this effect.

6. Conclusions

(1) Equatorial region VHF ionospheric scatter signals were usually stronger than their counterparts at temperate latitudes.

(2) *F*-region scatter propagation was observed only at nighttime over a 2580 km path.

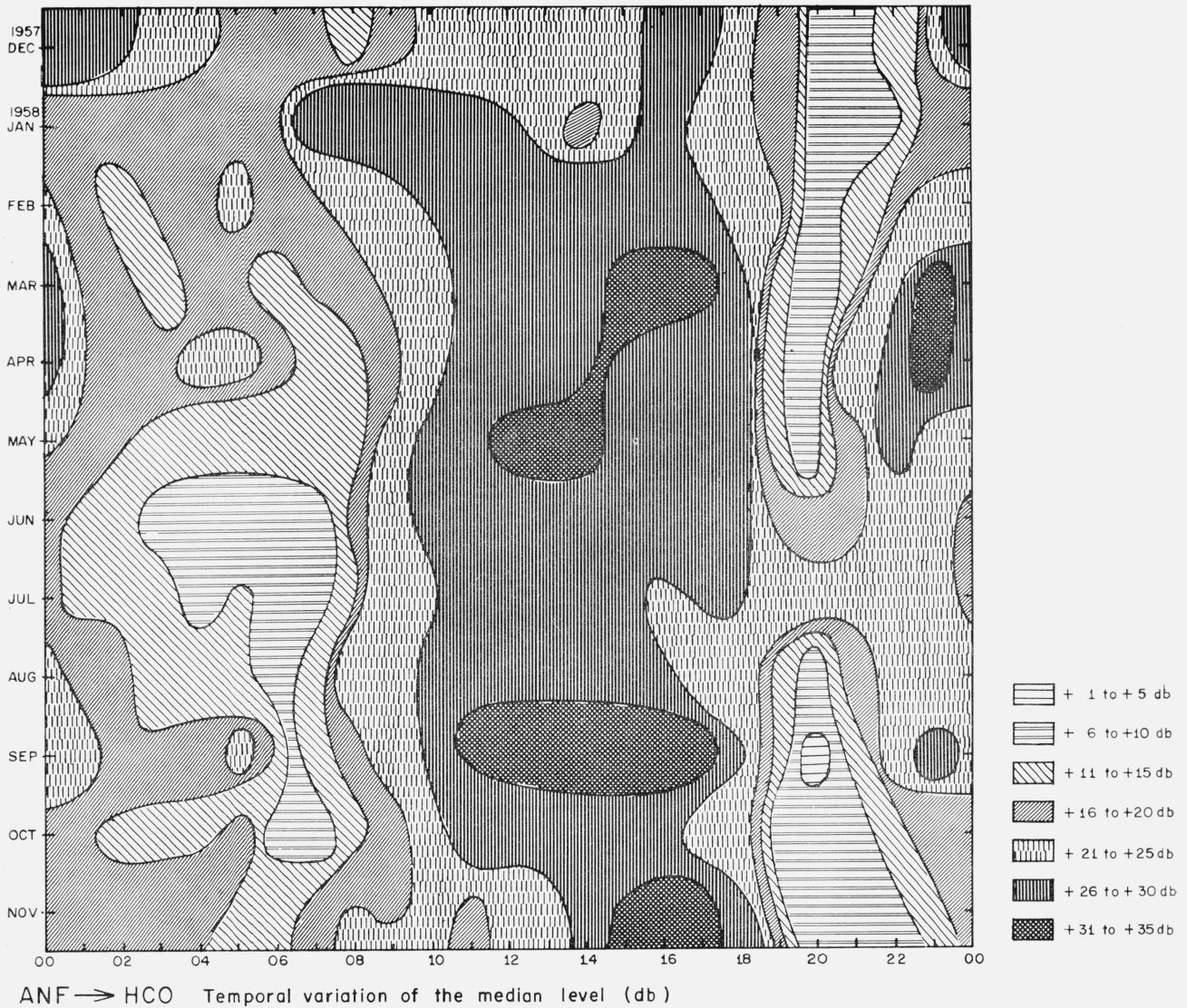(3) Strong *E*-region scatter signals may be obtained via irregularities associated with the equatorial

477

▨	+ 1 to + 5 db
▤	+ 6 to +10 db
▨	+ 11 to +15 db
▨	+ 16 to +20 db
▨	+ 21 to +25 db
▊	+ 26 to + 30 db
▨	+ 31 to + 35 db

ANF —→ HCO   Temporal variation of the median level (db)

FIGURE 18. *Contours showing the temporal and seasonal variation of the range of signal strength exceeded 50 percent of the time over the south path.*

electrojet. The irregularities were estimated to be at heights ranging from 95 to 110 km.

(4) *D*-region scattering, when resolvable, was usually stronger than its counterpart at temperate latitudes, except just at the magnetic equator in the daytime.

(5) *E*-region scattering at night usually exceeded in intensity the maximum signals observed over paths at temperate latitudes.

(6) *E*-region scatter signals propagated from a point 5° south of the magnetic equator were usually stronger than those propagated a comparable distance to the north, and were stronger at night than those propagated just at the magnetic equator.

(7) Strong scatter signals associated with blanketing sporadic *E* irregularities were observable on paths with midpoints to the north and south of the magnetic equator, but seemed to be excluded for a path with midpoint just at the magnetic equator.

(8) The effect of SID's was to reduce the intensity of signals scattered in the *E* region.

(9) There was little seasonal variation in the daytime, electrojet-propagated scatter signal.

This equatorial VHF forward scatter experiment represents the fulfillment of the original aspirations and recommendations for such a program by D. K. Bailey, who was also interested in the possibilities of scattering in the *F* region. We are grateful to him for those suggestions, and to R. C. Kirby for his contributions to the original planning and preparation of this IGY program. We are appreciative of the painstaking data analysis by K. W. Sullivan, B. B. Balsley, and their associates. The computer
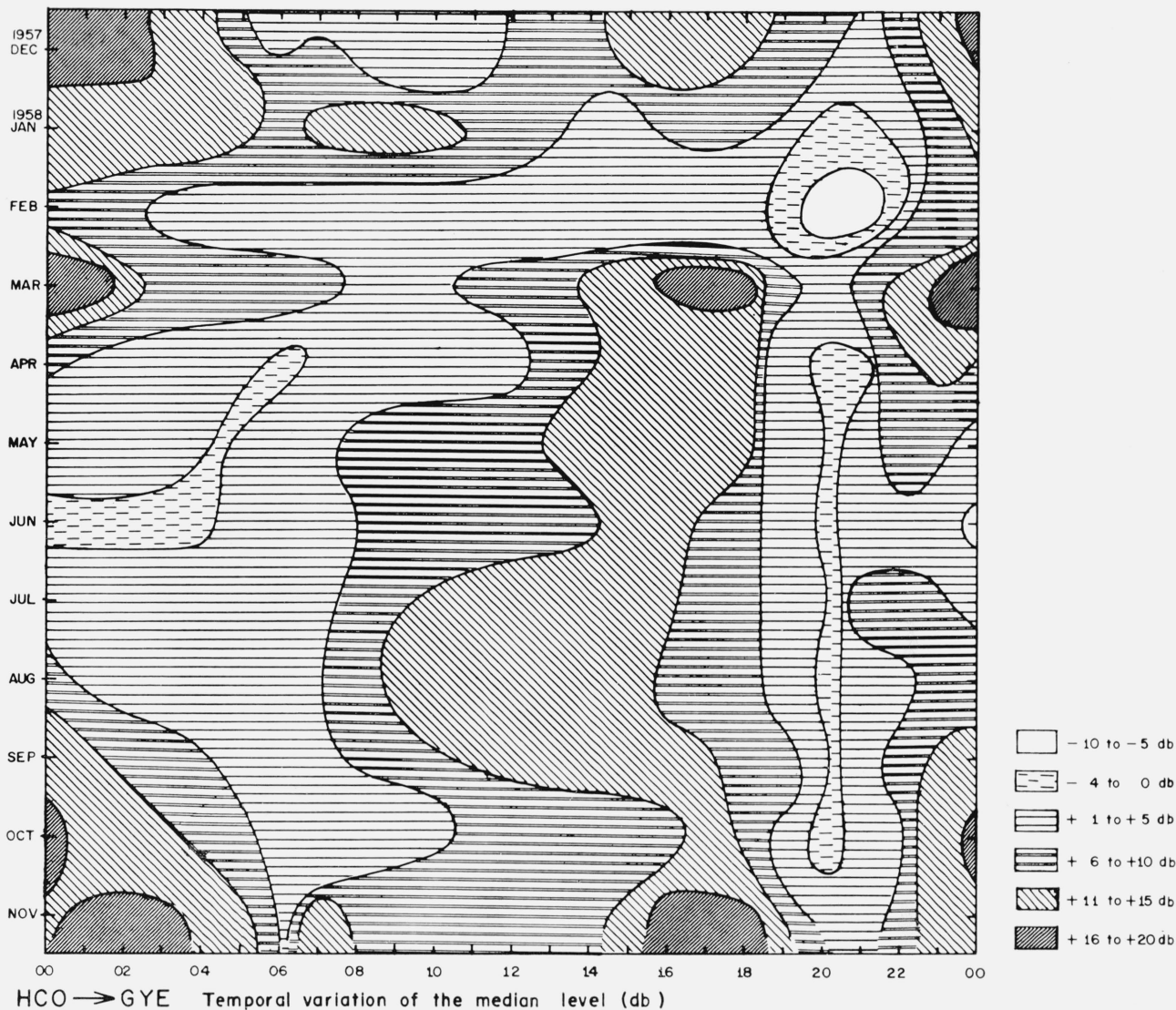
FIGURE 19. *Contours showing the temporal and seasonal variation of the range of signal strength exceeded 50 percent of the time over the north path.*

7. References

Bailey, D. K., R. Bateman, and R. C. Kirby (Oct. 1955), Radio transmission at VHF by scattering and other processes in the lower ionosphere, Proc. IRE **43**, 1181–1231.

Blair, J. C. (Apr. 1959), Frequency dependence of VHF ionospheric scattering, NBS Tech. Note No. 9.

Blair, J. C., R. M. Davis, Jr., and R. C. Kirby (Sept.–Oct. 1961), Frequency dependence of D-region scattering at VHF, J. Research NBS **65D** (Radio Prop.), No. 5, 417–425.

Bowles, K. L., B. B. Balsley, and R. Cohen (May, 1963), Field-aligned E-region irregularities identified with acoustic plasma waves, J. Geophys. Res. **68**, No. 9, 2485–2501.

Bowles, Kenneth, and Robert Cohen (Aug. 1957), NBS equatorial region VHF scatter research program for the IGY QST **41**, 11–15.

Bowles, Kenneth L., and Robert Cohen (1960), Studies of scattering phenomena in the equatorial ionosphere based upon VHF transmissions across the magnetic equator, in *Some Ionospheric Results Obtained during the International Geophysical Year*, W. J. G. Beynon, ed., pp. 192–194 (Elsevier).

Bowles, Kenneth L., and Robert Cohen (1962), A study of radio wave scattering from sporadic E near the magnetic equator, in *Ionospheric Sporadic E*, E. K. Smith, Jr., and S. Matsushita, eds., pp. 51–77 (Pergamon Press, London).

Bowles, K. L., R. Cohen, G. R. Ochs, and B. B. Balsley (1960), Radio echoes from field-aligned ionization above the magnetic equator and their resemblance to auroral echoes, J. Geophys. Res. **65**, 1853–1855.

Calvert, Wynne, and Robert Cohen (Oct. 1961), The interpretation and synthesis of certain spread-F configurations appearing on equatorial ionograms, J. Geophys. Res. **66**, 3125–3140.

Cohen, Robert, and Kenneth L. Bowles (Apr. 1961), On the nature of equatorial spread F, J. Geophys. Res. **66**, 1081–1106.

Cohen, Robert, and Kenneth L. Bowles (May, 1963), The association of plane-wave electron-density irregularities with the equatorial electrojet, J. Geophys. Res. **68**, No. 9, 2503–2525.

Cohen, Robert, Kenneth L. Bowles, and Wynne Calvert (Mar. 1962), On the nature of equatorial slant sporadic E, J. Geophys. Res. **67**, 965–972.

Farley, D. T., Jr. (Apr. 1, 1963), The two-stream instability as a source of irregularities in the ionosphere, Phys. Rev. Letters **10**, No. 7, 279–282.

Gates, David M. (Jul.–Aug. 1959), Preliminary results of the National Bureau of Standards radio and ionospheric observations during the International Geophysical Year, J. Research NBS **63D** (Radio Prop.), No. 1, 1–14.

Gray, Alvin M., and John N. Gorham (May 1, 1961), *Instruction Manual for NBS Laboratory Receiver*, (private communication).

Joint Technical Advisory Committee (1960), Radio transmission by ionospheric and tropospheric scatter, Proc. IRE **48**, 4–44.

Knecht, R. W., and R. E. McDuffie (1962). On the width of the equatorial E_s belt, in *Ionospheric Sporadic E*, E. K. Smith, Jr., and S. Matsushita, eds., pp. 215–218 (Pergamon Press, London).

Matsushita, S. (1951), Intense E_s ionization near the magnetic equator, J. Geomag. Geo. **3**, 44–46.

Smith, Ernest K., Jr., and James W. Finney (Mar. 1960), Peculiarities of the ionosphere in the Far East: A report on IGY observations of sporadic E- and F-region scatter, J. Geophys. Res. **65**, 885–892.

Southworth, M. P. (Feb. 1960), Nighttime equatorial propagation at 50 Mc/s: First results from an IGY amateur observing program, J. Geophys. Res. **65**, 601–607.

Tao, Kazuhiko, Junichi Asai, Akira Sakurazawa, Kazuaki Sawaji, and Makoto Yamaoka (Sept. 1961), Results of long experiments on long-distance (1,110 km) propagation in VHF bands, J. of the Radio Research Laboratories **8**, Nos. 38/39, 331–353.